Geometrical Similarities of the Orlov and Tuy Sampling Criteria and a Numerical Algorithm for Assessing Sampling Completeness

S. D. Metzler, *Member, IEEE,* J. E. Bowsher, *Member, IEEE,* and R. J. Jaszczak, *Fellow, IEEE*

***Abstract*—Tuy and others have derived a sufficiency condition for complete sampling using a cone-beam geometry. Herein, we express Tuy's cone-beam condition in the language and geometry of Orlov's condition for parallel-beam collimation. One may determine from this condition what volume is completely sampled. This inversion has been implemented in software. The software determines a lower bound on the completely sampled volume for arbitrary orbits.**

***Index Terms*—Conebeam, data sufficiency, Orlov, parallel-beam, pinhole, Tuy.**

I. Introduction

ORLOV'S condition is based on the set of vantage angles observed by parallel-beam collimation [1]. Tuy's condition is a condition on the relationship of points to the curve of the cone-beam's focal (source) point [2]. Tuy's condition is equivalent to Orlov's condition in the limit of infinite focal length [3]. We develop this relationship further by highlighting a geometrical similarity between Tuy's condition and Orlov's. This relationship is valid for finite focal lengths; our derivation does not restrict us to infinite focal lengths. We then describe a computational algorithm for determining the region that is completely sampled by the universal aperture [3] of the support for arbitrary orbits. This region is a lower bound on the region completely sampled by the orbit.

II. Sampling Criteria

A. Sampling Criteria for Parallel-Beam Collimation

Orlov derived in the context of electron microscopy the complete-sampling condition for three-dimensional reconstruction from parallel projection data [1]. He stated his condition geometrically: the curve of vantage angles on a unit sphere of directions must "have points in common with any arc of a great circle [1]." Orlov's condition was derived based on the assumption that the entire density function $f(x)$ is observed from the same set of vantage angles (i.e., untruncated parallel-beam collimation). Hence, one can use Orlov's condition to determine the completely sampled volume for a given parallel-beam orbit as follows: Determine the set of points that are untruncated throughout the orbit and then apply Orlov's criterion to the set of vantage angles for any point within that volume. Since parallel-beam collimators have translational symmetry (i.e., shift invariance), all points in the untruncated volume are seen by the same set of vantage angles. Orlov's criteria is a condition on the set of vantage angles seen by all points.

B. Sampling Criteria for Cone-Beam Collimation

Tuy and others have derived a completeness condition for cone-beam acquisitions [2], [4], [5]. The Tuy condition is also stated geometrically: "if on every plane that intersects the object there exists at least one cone-beam source (focal) point, then one can reconstruct the object [2], [5]." As with Orlov's condition, Tuy's condition assumes that the object is untrucated in each projection.

Cone-beam collimation approaches the translational invariance of parallel-beam collimation in the limit of infinite focal length. However, when the focal length is finite, the translational symmetry of the cone-beam collimator is broken. Consequently, the set of vantage angles provided by a given orbit varies from one point to another.

C. Geometrical Connection of Orlov's and Tuy's Conditions

We now endeavor to geometrically connect Orlov's condition to the Tuy condition. We do not make any assumptions about cone-beam focal length. Fig. 1 depicts the Tuy condition at a point $\vec{x}$ in the completely sampled volume. One plane through the point is indicated by the dotted line. The normal to the plane is unit vector $\hat{\beta}$. The curve of focal points $\vec{\Phi}$ is represented as a solid ellipse. The curve intersects the plane at $\vec{\Phi}_0$ and $\vec{\Phi}_1$. The Tuy condition requires the curve to intersect every plane through each point $\vec{x}$ in the completely sampled volume. The set of all planes through $\vec{x}$ corresponds to the set of all values of $\hat{\beta}$. Although there may be multiple intersections, only one is needed: $\vec{\Phi}_0$.

Orlov's condition for parallel-beam collimation involves the set of angles from which $f(x)$ is viewed (i.e., the set of vantage angles). For cone-beam collimation, the vantage angle $\vec{S}$ is the vector from $\vec{x}$ to $\vec{\Phi}_0$. $\hat{S_N}$ is the normalized (unit) vantage angle.

Manuscript received January 28, 2003; revised May 23, 2003. This work was supported by the National Cancer Institute of Biomedical Imaging and Bioengineering of the National Institutes of Health under Grants R01-CA-76006, R01-EB-00211, and R21-EB-001543, and by the Biological and Environmental Research Program (BER), U.S. Department of Energy, Grant DE-FG-02-96ER62150.

S. D. Metzler and J. E. Bowsher are with the Department of Radiology, Duke University Medical Center, Durham, NC 27710 USA (e-mail: metzler@duke.edu).

R. J. Jaszczak is with the Department of Radiology, Duke University Medical Center, Durham, NC 27710 USA, and also with the Department of Biomedical Engineering, Duke University, Durham, NC 27710 USA.

Digital Object Identifier 10.1109/TNS.2003.817385

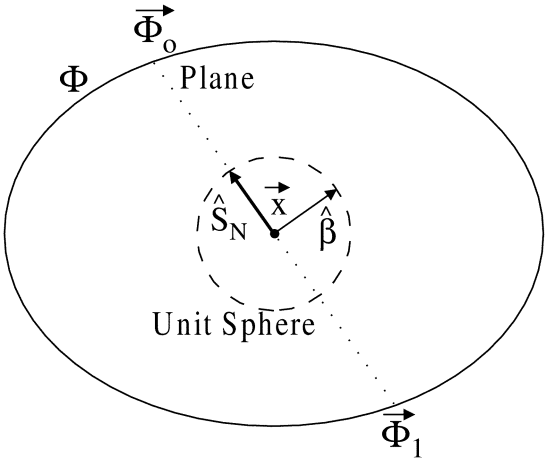

Fig. 1. A plane (dotted line) with normal $\hat{\beta}$ intersects the object at $\vec{x}$. The plane also intersects the path $\vec{\Phi}$ of the focal-point curve (solid ellipse) at $\vec{\Phi}_0$ and $\vec{\Phi}_1$. The unit vector specifying the vantage angle is $\hat{S_N}$. A unit sphere for specifying all possible directions (indicated by the dashed circle) is centered at $\vec{x}$. The unit direction vectors $\hat{\beta}$ and $\hat{S_N}$ have their origin at $\vec{x}$.

To establish the connection between Orlov's condition and Tuy's condition, we define the plane $\vec{P}$ through $\vec{x}$ whose normal is $\hat{\beta}$

$$\vec{P} = \left(\vec{x'} - \vec{x}\right) \cdot \hat{\beta} = 0. \tag{1}$$

All points $\vec{x'}$ that satisfy (1) are in $\vec{P}$.

The intersection of the plane $\vec{P}$ with the curve $\Phi(\vec{\lambda})$ occurs at $\vec{\Phi}_0$

$$\left(\vec{\Phi}_0 - \vec{x}\right) \cdot \hat{\beta} = 0. \tag{2}$$

The vantage angle, $\vec{S}$, is the vector from $\vec{x}$ to $\vec{\Phi}_0$

$$\vec{S} = \vec{\Phi}_0 - \vec{x}. \tag{3}$$

The normalized vantage angle is

$$\hat{S_N} = \frac{\vec{S}}{|\vec{S}|} = \frac{\vec{\Phi}_0 - \vec{x}}{|\vec{\Phi}_0 - \vec{x}|}. \tag{4}$$

By (2), S_N is perpendicular to $\hat{\beta}$ since its dot product with $\hat{\beta}$ is zero.

Each great circle is the intersection of a sphere with a plane that contains the center of the sphere. There is a one-to-one mapping between unit great circles centered at $\vec{x}$ and planes through $\vec{x}(\vec{x} \cdot \hat{\beta}, \hat{\beta})$ where the ordered pair $(\vec{x} \cdot \hat{\beta}, \hat{\beta})$ uniquely specifies a plane by its normal $\hat{\beta}$ and its displacement from the origin $\vec{x} \cdot \hat{\beta}$ along the direction $\hat{\beta}$. If the curve of focal points has multiple intersections, all intersections correspond degenerately to the same plane and great circle.

If a plane defined by $\hat{\beta}$ and $\vec{x} \cdot \hat{\beta}$ intersects the curve of the focal point $\vec{\Phi}$, then the corresponding unit great circle (i.e., the great circle that is in that plane and that is centered at $\vec{x}$) is intersected by the direction vector $\hat{S_N}$ specifying the vantage angle. The vantage-angle vector $\hat{S_N}$ is a vector in the plane $\vec{P}$ with origin $\vec{x}$. Since the great circle and $\hat{S_N}$ are in the same plane, they have the same origin, and the magnitude of $\hat{S_N}$ equals the circle's radius, $\hat{S_N}$ is the displacement vector from $\vec{x}$ to a point on the great circle defined by $\hat{\beta}$. Consequently, if a plane through $\vec{x}$ intersects the curve of focal points, the corresponding great circle is also intersected. Therefore, for all planes through $\vec{x}$ to intersect the focal curve, all unit great circles centered at $\vec{x}$ must be intersected, and for all great circles centered at $\vec{x}$ to be intersected, all planes through $\vec{x}$ must intersect the focal curve.

Thus, Tuy's condition [2] may be stated as follows, using the geometrical language of Orlov: For all voxels in the completely sampled volume, the set of vantage angles on a unit sphere of directions, from each voxel to each point on the curve of focal points, must "have points in common with any arc of a great circle [1]" surrounding that voxel. Based on this restatement of Tuy's condition, we introduce a numerical algorithm for determining the largest completely sampled region (LCSR) corresponding to a given cone-beam or parallel-beam orbit.

The Tuy condition is for untruncated projections. In order to establish a set of untruncated projections, we utilize the concepts of support, universal aperture, and LCSR.

Support: Let the support be the set of voxels over which the imaged object $f(x)$ may be nonzero [i.e., $f(x)$ is known to be zero outside the support].

Universal Aperture for Cone-Beam Collimation: In analogy to the universal aperture concept for parallel-beam collimation [3], we define the universal aperture for cone-beam collimation for a region of space B to be the set of focal points for which B is not truncated. In the limit of infinite focal length (parallel-beam collimation), this is equivalent to the set of projection directions for which B is not truncated since all voxels within the support experience the same vantage angle.

LCSR: We define the LCSR to be the largest subset of the support for which the universal aperture meets Tuy's condition. That is, the LCSR is the largest subset of the support such that the universal aperture of focal point locations intersects every plane that intersects that subset of the support.

We apply our numerical algorithm to the universal aperture of the support; B corresponds to the support. This assures that the object is untruncated (since the object is zero outside the support) for all views that are considered (all views in the universal aperture). Since the nonzero voxels are contained within the support, the density function can be reconstructed within the LCSR [2].

III. Algorithm for Calculating Completely Sampled Volumes

An algorithm has been developed to determine the LCSR. A voxelized representation of the volume to be evaluated is created. Then a set of collimator models is constructed to simulate the positions, orientations and spatial extents of the collimators. For example, a single parallel-beam collimator following an orbit that includes m projection views would be represented by m collimator models. Two collimators with m and n projection views, respectively, would be represented by $m + n$ collimator models. For each voxel, a digitized version of the vantage points of the voxel are determined from the set of collimator

models. The digitized vantage curve (DVC) is then evaluated to determine if any great circles can exist on the Orlov sphere without intersecting the vantage curve.

This algorithm has been implemented in C++ using Object-Oriented programming techniques [6]. When started, the program allocates and initializes a boolean matrix representing the voxelized volume to consider. It then reads one or several orbit files and constructs a set of collimator representations. All detector representations obey an *abstract interface* that determines if a given voxel is within the field-of-view of the collimator and the vantage angles for that voxel [6].

The use of an abstract interface makes it possible to model multiple collimator types simultaneously and extend the program to consider new collimator types without any change to the algorithm. The new collimator simply needs to implement this interface.

A. Vantage Curve Digitization

The DVC for each voxel is fully determined and evaluated before the next voxel is considered in order to reduce the required memory. The vantage curve is stored in digital form by using a two-dimensional grid to represent the polar angle, θ, and the azimuthal angle, ϕ, of each vantage point. The grid is boolean so that *true* represents a coordinate pair (θ, ϕ) for an observed vantage point (OVP) and *false* represents an unobserved vantage point (UVP). An odd, but variable, number of rows (N_{rows}) were used to represent θ so that the central row corresponded to the equator. An even number of columns (N_{cols}) represented ϕ for the matrix so that each column has a well-defined complementary column (CC), which represents the azimuthal values on the opposite side of the sphere. The CC is 180° and $N_{\text{cols}}/2$ bins away from its pair. A schematic representation of a DVC is shown in Fig. 2.

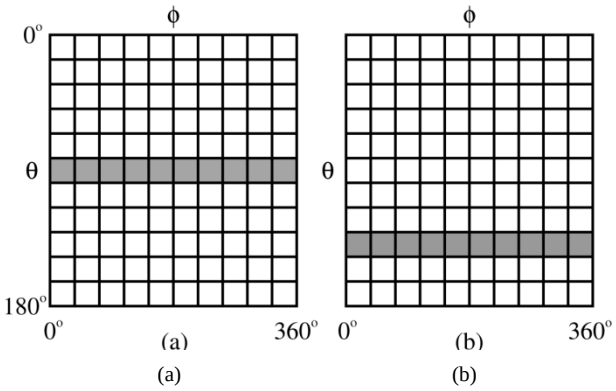

Fig. 2. Digital (binned) representation of vantage curves. The digital representations of the vantage curves for 360° orbits of a parallel-beam collimator and a slant-hole collimator are shown schematically as matrices in (a) and (b), respectively. Observed vantage points (OVP) are shaded. Unobserved vantage points (UVP) are unshaded. The equator is shaded in (a), but completely unshaded in (b).

B. Vantage Curve Evaluation

After all the projection views have been considered for a voxel, the vantage curve is complete and is evaluated to determine if any great circles can exist on the sphere without intersecting the vantage curve. The parameterization of a generic great circle (Fig. 3) can be found by considering that the points with the minimum and maximum z values are

$$\hat{r}_{\max} = (\sin\theta_{\text{m}}\cos\phi_{\text{m}},\ \sin\theta_{\text{m}}\sin\phi_{\text{m}},\ \cos\theta_{\text{m}})$$
$$\hat{r}_{\min} = (-\sin\theta_{\text{m}}\cos\phi_{\text{m}},\ -\sin\theta_{\text{m}}\sin\phi_{\text{m}},\ -\cos\theta_{\text{m}}) \quad (5)$$

where θ_{m} is the value of θ for the circle's maximum z point.

The normal to the circle is $\hat{\beta}$

$$\hat{\beta} = (\cos\theta_{\text{m}}\cos\phi_{\text{m}},\ \cos\theta_{\text{m}}\sin\phi_{\text{m}},\ -\sin\theta_{\text{m}}). \quad (6)$$

The normal can be used to determine the basis vector orthogonal to $\hat{r}_{\max}$, $\hat{r}_{\min}$, and $\hat{\beta}$

$$\hat{b} = \hat{r}_{\max} \times \hat{\beta} = -\hat{x}\sin\phi_{\text{m}} + \hat{y}\cos\phi_{\text{m}}. \quad (7)$$

Any point on the great circle can be parameterized as

$$\hat{S_N} = \alpha\hat{r}_{\max} + \beta\hat{b}. \quad (8)$$

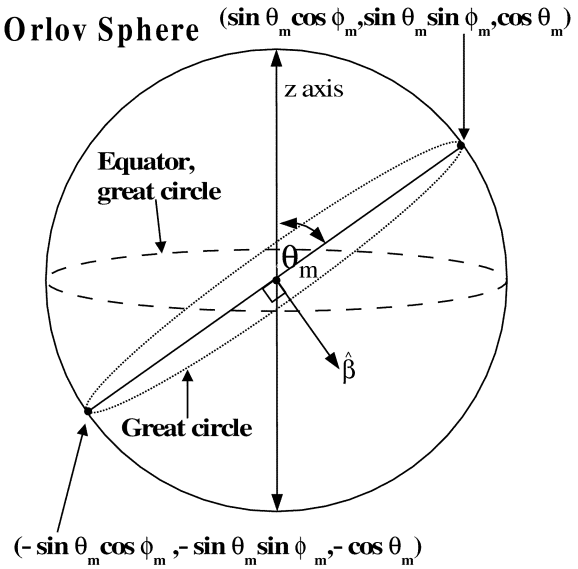

Fig. 3. Generic great circle on an Orlov sphere. The point $(\sin\theta_{\text{m}}\cos\phi_{\text{m}},\ \sin\theta_{\text{m}}\sin\phi_{\text{m}},\ \cos\theta_{\text{m}})$ has the maximum value of z on this curve. The point $(-\sin\theta_{\text{m}}\cos\phi_{\text{m}},\ -\sin\theta_{\text{m}}\sin\phi_{\text{m}},\ -\cos\theta_{\text{m}})$ has the minimal value of z on this curve. The normal to the plane of this great circle is $\hat{\beta}$.

Since $|\hat{S_N}| = |\hat{r}_{\max}| = |\hat{b}| = 1$, and $\hat{r}_{\max}$ and $\hat{b}$ are orthogonal

$$\alpha^2 + \beta^2 = 1. \quad (9)$$

Letting $\alpha = \cos\gamma$ and $\beta = \sin\gamma$

$$\hat{S_N} = (\cos\gamma\sin\theta_{\text{m}}\cos\phi_{\text{m}} - \sin\gamma\sin\phi_{\text{m}}\ \cos\gamma\sin\theta_{\text{m}}\sin\phi_{\text{m}} + \sin\gamma\cos\phi_{\text{m}},\ \cos\gamma\cos\theta_{\text{m}}) \quad (10)$$

where θ_{m} and ϕ_{m} are the coordinates of the point of maximum z on the curve and γ parameterizes the curve.

Equation (10) is used to evaluate if any great circles can exist on the sphere without intersecting the vantage curve. The matrix representing the DVC is evaluated for intersections by using each element in the top half of the matrix ($\theta < 90°$) as $\hat{r}_{\max}$ for

a particular trial great circle. Equation (10) is then used to determine all the other element locations in the DVC that are on the same trial great circle by varying γ. This is done by determining the value of $\cos\gamma$ for each row of the DVC. In general there are two solutions for γ each row. At the extremes (i.e., the maximum and minimum points of the circle, where $\cos\gamma = \pm 1$), the two solutions are degenerate. There are no solutions for rows where $|\cos\gamma| > 1$. The element locations in the DVC are compared with the OVPs to determine if there are intersections (i.e., check the OVPs for *true*). If an intersection is found, the trial great circle is not allowed and the next trial great circle is checked by choosing the next $\hat{r}_{\max}$.

Although (10) gives the form of the generic great circle, it can be computationally intensive to apply to all points on the digitized curve using the method described above. Several simplified cases are checked before the generic method is used. First, the number of OVPs found must be greater than the lesser of N_{rows} and $N_{\text{cols}}/2$. Otherwise, a great circle can be drawn. Second, the equator is checked to verify that a great circle cannot be drawn through the equator. This check is satisfied if a single observed point is found (Fig. 2(b) fails this check). Third, the azimuthal columns are checked to verify that a great circle cannot be drawn longitudinally. This check is satisfied if a single observed point is found in a column or its CC. Fourth, the central row (equator) is checked to see if enough of it is filled in to exclude all great circles. This last case would require that a contiguous section of the equator at least as large as half of the circumference be marked as observed (Fig. 2(a) passes this check).

C. Examples

The program has been tested using parallel-beam collimators, slant-hole collimators, and cone-beam/pinhole collimators. Example volumes are described below.

1) Parallel-Beam Collimators With Circular Orbits: Parallel-beam collimators with untilted circular 360° orbits have been evaluated on a 64^3 grid of 0.712-cm-wide voxels and give cylindrical LCSRs, as expected. A transaxial slice of an LCSR is shown in Fig. 4(a). For this LCSR, the gamma camera dimensions were 45.6 cm transaxially and 22.8 cm axially. The radius of rotation was 30.0 cm.

The LCSR of a parallel-beam collimator following a 360° circular orbit depends only on the detector dimensions and not the orbit dimensions. That volume is cylindrical with magnitude $\pi w^2 d/4$, where w is the transaxial width of the detector and d is the axial depth of the detector. The LCSR volume predicted by the formula is 37 157 cm^3. The volume determined by the program was 38 670 cm^3, which is larger than expected by 4%, presumably because of binning effects.

Fig. 4(b) shows the LCSR for a semicircular (180°) orbit of a parallel-beam collimator. It is asymmetric. Halfway through the 180° orbit, the camera has a view to the right. The ROR was 10.0 cm. The calculated volume was 14 761 cm^3. The expected volume was

$$\frac{w^2}{4}\sin^{-1}\frac{20}{w} + \frac{20}{4}\sqrt{w^2 - 20^2} + \frac{20^2}{8}\pi = 13\,634\ \text{cm}^3. \quad (11)$$

2) Cone-Beam/Pinhole Collimators: A cone-beam/pinhole collimator model has been implemented for the algorithm.

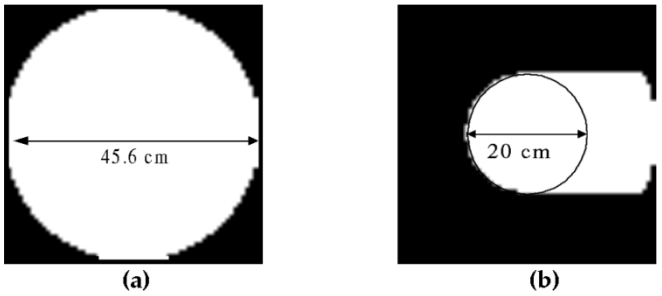

Fig. 4. Transaxial slice of the LCSR for parallel-beam collimator with a circular orbit. The volume is cylindrical with a diameter of 45.6 cm.

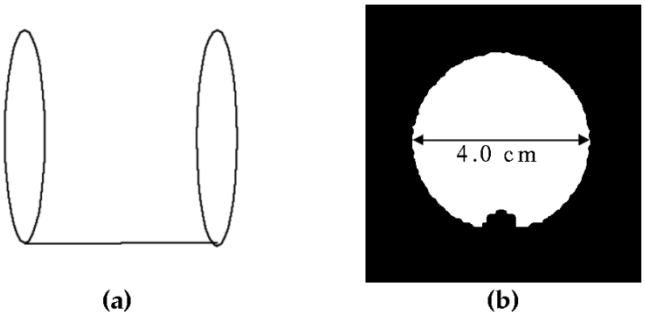

Fig. 5. (a) Orbit [left] of the focal point of a cone-beam/pinhole collimator and (b) transaxial slice [right] of the LCSR for that orbit.

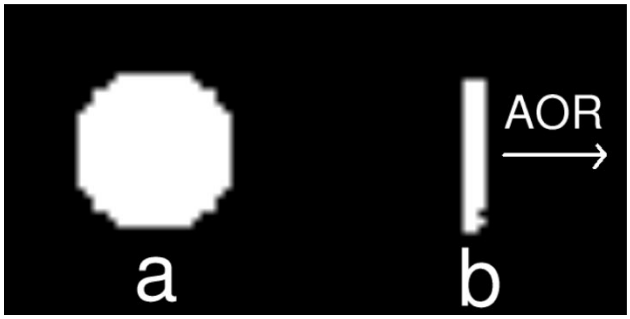

Fig. 6. LCSR for helical plus half-circle pinhole-collimator orbit. (a) Transaxial and (b) sagittal slices through the LCSR are shown. The volume is nearly cylindrical, except for defects at the ends (b, bottom), where the valid volume depends on the initial angle of acquisition, and except for binning effects. The axial translation of the orbit is 1.28 cm, which corresponds to two bins. The volume is three bins wide axially due to edge effects and centering.

A collimator with an opening angle of 180° has been tested with the following orbit: two 128-view circular orbits (ROR = 2.0 cm) connected by a 4.0 cm linear (axial) scan [7]. Although an opening angle of 180° is unrealistic in practice, it is useful for avoiding truncation in this example. The orbit (left) and the LCSR are shown in Fig. 5. The calculated volume is 48.5 cm^3, compared with the 50.3 cm^3 volume of the cylinder outlined by the orbit. Much of the difference is due to the defect at the bottom of the LCSR, nearest the axial translation of the focal point. It is the closest to the focal point during the axial translation. The pinhole-collimator has also been tested with a 192-view helical orbit and gives a nearly cylindrical LCSR using a 64^3 grid of 0.712 cm-wide voxels (Fig. 6). The orbit included a 128-view helical orbit with a 10 cm ROR traversing 1.28 cm along the axis of rotation followed by a 64-view half-circular orbit at the far end of the helix [8]. The defects in

the cylinder are at the ends, as expected because of the strong dependence on the initial orientation of the camera. The total volume determined by the program was 368 cm^3.

IV. Discussion

The completeness condition for ideal parallel-beam collimators may be evaluated for the vantage angles of any single point, because of the symmetry of the collimator. That is because, for parallel-beam collimators, the set of vantage angles is the same for all points in the untruncated volume. There is thus a translational invariance in parallel-beam collimation. Cone-beam collimation breaks the symmetry of the parallel-beam collimator. However, Tuy's condition has been shown to be geometrically equivalent to the following condition: For a unit sphere of directions surrounding each voxel in the completely sampled volume, the curve of vantage angles (created by the motion of the focal point) must "have points in common with any arc of a great circle [1]" on the unit sphere surrounding each voxel in the completely sampled volume. For cone-beam/pinhole geometries, the curve of vantage angles will differ for different voxels, whereas for parallel-beam geometries the curve of vantage angles is the same for all voxels. For cone-beam/pinhole geometries, as the focal point goes to infinity, the curve of vantage angles becomes the same for all voxels, giving the parallel-beam case [3] (i.e., giving Orlov's theorem). By expressing Tuy's condition in the terms of the geometrical language of Orlov's condition, we highlight this similarity between the two conditions. This relationship is valid for cone-beam collimation with finite focal length. This geometrical picture is the basis for the numerical algorithm presented here for computing the LCSR corresponding to a given orbit. This algorithm is equally applicable to parallel-beam and cone-beam/pinhole geometries because of the underlying, same geometrical picture for Orlov's parallel-beam and Tuy's cone-beam/pinhole conditions.

The LCSR as defined here is a lower bound on the region that is completely sampled by a set of projections for two reasons: 1) Tuy's condition is a sufficiency condition and 2) the completely sampled region may be extended by projections outside of the universal aperture. Since all nonzero activity is assumed to be within the support and only untruncated projections of the support are used, the activity distribution is, by assumption, untruncated for all projection views used so that the Orlov and Tuy conditions apply. The LCSR may then be reconstructed as a subset of the support.

An alternative to the algorithm and corresponding objective presented here would be to consider the common volume [9] (i.e., the volume that is not truncated by any projection views) and then determine the largest completely sampled volume that is a subset of the common volume. In this formulation, all nonzero activity would be assumed to be contained within the common volume so that the LCSR can be reconstructed. A disadvantage of this alternative algorithm is that the common volume may be severely limited by a small number of projection views.

The current algorithm has successfully determined the LCSR in cases that are easily verified intuitively. It has been used to study the more complex scenarios of pinhole collimators following a helical orbit. This technique may be useful for studying complete orbits and understanding sampling artifacts for complex projection acquisitions.

Algorithm optimization has been an important issue for timely completion of the volume calculation. For the 64^3 voxel representation used herein, the approximate computation time on an AMD 1.0 GHz processor is 5 min, but is sensitive to the complexity of the orbit. This time is typically dominated by evaluations that require the full use of (10) instead of one of the simpler evaluations that were mentioned in the same section. One optimization would be to apply the test to parallel-beam data at just one point in the untruncated volume. However, this would break the abstraction model of the program for only a factor of 2 gain in computation time. Further optimizations would involve improving the implementation of the check using (10). One way this could be done would be to pre-compute the great circles for each row of the matrix. Since the columns represent equally spaced azimuthal regions, the curve can then be translated quickly on the fly. It is also possible that other simplifying cases can be added to more quickly evaluate for great circles. These additional optimizations are not currently a significant issue because of the fast computation time that has already been achieved.

Orlov's condition assumes continuous angular sampling and infinitesimal sampling bins. Both of these conditions are invalid in realistic acquisitions. By Nyquist's theorem, there are limitations in reconstruction resolution due to discrete sampling.

The algorithm described herein uses a discrete matrix to determine the DVC and hence the LCSR. The size of the grid needs to match the angular sampling of the orbit. If N_{cols} and N_{rows} in the matrix are too small, an incomplete orbit may appear complete. If N_{cols} and N_{rows} is too large, there would be unintended UVPs, allowing a complete orbit to appear incomplete.

A useful approach to this problem may be to construct approximately continuous orbits from discrete sampling points. This may more closely match the continuous nature of the Orlov and Tuy conditions. A possible solution in this direction is to use a large matrix in the DVC and to finely sample between discrete sampling points if they are within a certain user-specified angular distance on the unit sphere. A segment of a great circle, which is the shortest path between the two points, could be used in order to make a continuous arc. The continuous arc could then be very finely sampled in order to determine the OVPs and fill the DVC.

By using the algorithm, it may be possible to determine if the composite sampling from different collimator types is complete even if the individual sampling from each collimator is not complete. Since parallel-beam collimators are cone-beam collimators with infinite focal length (cone-beam collimators are not parallel-beam collimators), it seems reasonable, although unproven as far as we know, that combined orbits of parallel-beam and cone-beam collimation can be evaluated by the algorithm proposed here. Experimentally, combined parallel-beam and cone-beam projection data have been reconstructed to produce data without sampling artifacts [10], [11]. However, in these experiments, the parallel-beam data alone was complete.

Medical applications of CT may involve truncated projections. However, for CT applications in which projections are not truncated, this technique for computing the LCSR for SPECT

acquisitions may be applied to CT without modification to the algorithm. For CT, the line integral of attenuation is sampled at a set of focal-point positions, similar to the case of cone-beam/pinhole SPECT, where the line integral of emission activity is sampled. The existing cone-beam/pinhole collimator model can be used to determine the set of vantage angles sampled by CT. These line integrals determine the LCSR without change to the program.

V. Conclusion

Tuy's condition is geometrically equivalent to the following condition: For all voxels in the completely sampled volume, the set of vantage angles on a unit sphere of directions, from each voxel to each point on the curve of focal points, must "have points in common with any arc of a great circle [1]" surrounding that voxel. This relationship is valid for cone-beam collimation with finite focal length.

An algorithm based on this Orlov-like statement of Tuy's condition has been described. The algorithm determines a completely sampled volume. Examples of its application have been shown. The examples agree with expectation in all cases that were examined.

Acknowledgment

The authors would like to thank the anonymous reviewers for insightful comments on and suggestions for this paper.

References

[1] S. S. Orlov, "Theory of three dimensional reconstruction. I. Conditions for a complete set of projections," *Sov. Phys. Crystallogr.*, vol. 20, no. 3, pp. 312–314, 1975.

[2] H. K. Tuy, "An inversion formula for cone-beam reconstruction," *SIAM J. Appl. Math.*, vol. 43, no. 3, pp. 546–552, 1983.

[3] M. Defrise, R. Clack, and D. W. Townsend, "Image reconstruction from truncated, two-dimensional, parallel projections," *Inv. Prob.*, vol. 11, no. 2, pp. 287–313, 1995.

[4] A. A. Kirillov, "On a problem of I.M. Gel'fand," *Sov. Math. Dokl.*, vol. 2, pp. 268–269, 1961.

[5] B. D. Smith, "Image reconstruction from cone-beam projections: Necessary and sufficient conditions and reconstruction methods," *IEEE Trans. Med. Imaging*, vol. MI-4, no. 1, pp. 14–25, Mar. 1985.

[6] R. C. Martin, *Designing Object-Oriented C++ Applications Using the Booch Method*. Englewood Cliffs, NJ: Prentice-Hall, 1995.

[7] B. D. Smith, "Cone-beam tomography recent advances and a tutorial review," *Opt. Eng.*, vol. 29, no. 5, pp. 524–534, 1990.

[8] K. C. Tam, S. Samarasekera, and F. Sauer, "Exact cone beam CT with a spiral scan," *Phys. Med. Biol.*, vol. 43, pp. 1015–1024, 1998.

[9] R. Clack, P. Christian, M. Defrise, and A. Welch, "Image reconstruction for a novel SPECT system with rotating slant-hole collimators," in *Proc. 1994 Conf. Rec. IEEE Nuclear Science Symp. Medical Imaging Conf.*, Norfolk, VA, Nov. 1994, pp. 1948–1952.

[10] R. J. Jaszczak, J. Li, H. Wang, and R. E. Coleman, "Three-dimensional SPECT reconstruction of combined cone beam and parallel beam data," *Phys. Med. Biol.*, vol. 37, pp. 535–548, 1992.

[11] M. Defrise and R. Clack, "Filtered backprojection reconstruction of combined parallel beam and cone beam SPECT data," *Phys. Med. Biol.*, vol. 40, pp. 1517–1537, 1996.